The Cryosphere, 3, 231–243, 2009
www.the-cryosphere.net/3/231/2009/

The Cryosphere

Mapping glaciers in Jotunheimen, South-Norway, during the "Little Ice Age" maximum

S. Baumann[1], **S. Winkler**[1], **and L. M. Andreassen**[2]

[1]Department of Geography, Physical Geography, University of Wuerzburg, Wuerzburg, Germany
[2]Norwegian Water Resources and Energy Directorate (NVE), Oslo, Norway

Received: 16 June 2009 – Published in The Cryosphere Discuss.: 29 June 2009
Revised: 23 November 2009 – Accepted: 24 November 2009 – Published: 1 December 2009

Abstract. The maximum glacier extent during the 'Little Ice Age" (mid 18th century AD) in Jotunheimen, southern Norway, was mapped using remote sensing techniques. Interpretation of existing glaciochronological studies, analysis of geomorphological maps, and own GPS-field measurements were applied for validation of the mapping. The length of glacier centrelines and other inventory data were determined using a Geographical Information System (GIS) and a Digital Elevation Model. "Little Ice Age" maximum extent for a total of 233 glaciers comprising an overall glacier area of about 290 km^2 was mapped. Mean length of the centreline was calculated to 1.6 km. Until AD 2003, the area and length shrank by 35% and 34%, respectively, compared with the maximum "Little Ice Age" extent.

1 Introduction

Investigations of the glacier maximum extent during "Little Ice Age" (LIA) in South Norway have, until recently, mainly been carried out as locally focused studies on selected glaciers (e.g. Fægri, 1948; Hoel and Werenskiold, 1962; Matthews, 1977, 2005; Erikstad and Sollid, 1986; Bogen et al., 1989; Winkler, 2001). These investigations included dating of moraines, e.g. by application of lichenometry, and mapping of selected glaciers and glacier forelands. Previous studies have mainly focused on the region of Jostedalsbreen and a number of individual glaciers in Jotunheimen, e.g. Storbreen in Visdalen.

Glaciers offer a high potential to serve as key indicators for climate change (IPCC, 2007). In this context, a detailed knowledge of glacial chronology during the later Holocene is important as it serves as opportunity to verify forecasts and simulations of future glacier behaviour. Furthermore, and especially in Norway, knowledge of the behaviour of glaciers and their response to changes in climate has a practical meaning, because 98% of the domestic electricity is produced using hydropower and 15% of the exploited runoff is derived from glacierized river basins (Andreassen et al., 2005).

Mapping the LIA maximum glacier extent by conventional field work is time consuming. It is, therefore, usually applied to investigate selected glaciers rather than a large sample of glaciers or a whole region. By investigating larger regions, however, a robust regional trend can potentially be detected to avoid – or at least minimise – misinterpretations of specific behaviours of individual "key"-glaciers as representative. To study a whole region with a large number of individual glaciers, many difficult to access on the ground, remote sensing provides a practicable alternative. Studies in other regions have already demonstrated the potential of satellite imagery as an efficient tool for mapping of maximum LIA extents of glaciers on a regional scale (Solomina et al., 2004; Csatho et al., 2005; Paul and Kääb, 2005; Wolken, 2006; Paul and Svoboda, 2009).

The aim of this study was to reconstruct the glacier area during LIA maximum in Jotunheimen, and to create a glacier inventory for the LIA maximum. The data were used to analyze the glacier area change from LIA maximum until AD 2003, and to detect any possible spatial variability in glacier behaviour in this region.

Correspondence to: S. Baumann
(sabine.baumann@uni-wuerzburg.de)

Published by Copernicus Publications on behalf of the European Geosciences Union.

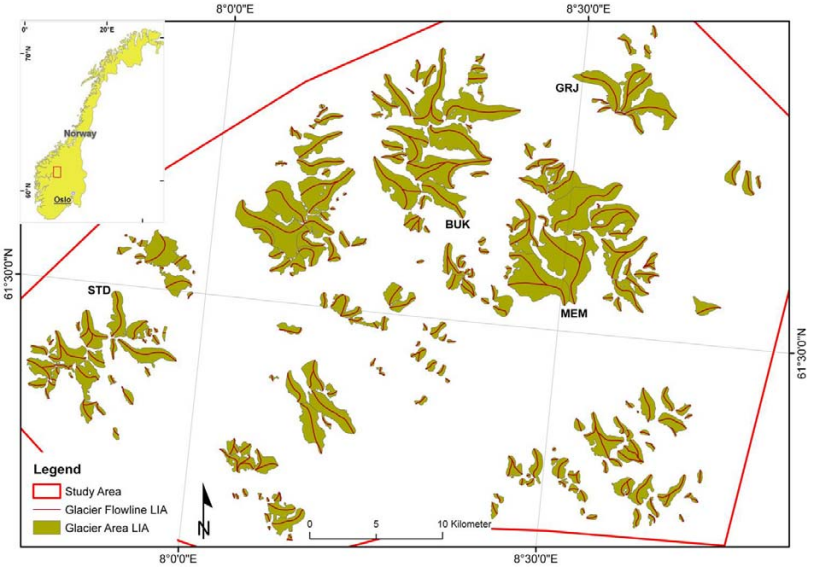

Fig. 1. Location of the study area Jotunheimen (inset) and glaciers ($>0.01\,km^2$) with flowlines during the LIA maximum. Letter codes denote: STD=Styggedalsbreen, BUK=Bukkeholsbreen, GRJ=Grjotbreen, MEM=Memurubreen. (Inset map: ESRI Templates).

2 Study area

The study area of Jotunheimen is located in central South Norway (61.5° N; 8.3° E) (Fig. 1). It has a high-alpine character and the highest points of Norway are located here (Galdhøpiggen 2469 m a.s.l.; Glittertind 2464 m a.s.l.). The present glaciers (i.e. AD 2003) are mostly small individual valley-type and cirque-type glaciers, separated by steep rock-walls and range from about 1300 to 2300 m a.s.l. (Andreassen et al., 2008). Long-term recorded mass balance along a West-East profile in southern Norway reveals a strong gradient in mass balance with decreasing mass turnover towards the more continental drier interior (e.g. Østrem et al., 1988).

The study area lies in a transitional zone between maritime and continental climate and represents the most continental glacier area in southern Norway (Østrem et al., 1988).

3 Timing of the LIA maximum in Jotunheimen

In contrast to Jostedalsbreen to the West, there are no historical documents or images of the glacier area of Jotunheimen that would allow a precise dating of the LIA maximum. Øyen (1893) and Hoel and Werenskiold (1962), respectively, report only a vague eyewitness story about the maximum extent of Storbreen, but no clear evidence that could be used for a distinct timing of the LIA maximum. Therefore, existing reconstructions of the glacial chronology in Jotunheimen prior to the first scientific measurements and historical photo-record around AD 1900 are primarily based on lichenometry, supported by ^{14}C-datings, lake sediment analysis, mire and colluvial profiles etc. (e.g. Matthews, 1974, 1975, 1977, 2005; Innes, 1985; Erikstad and Sollid, 1986; Winkler, 2001; Matthews and Dresser, 2008). These studies suggest that the timing of the culmination of the LIA in Jotunheimen falls roughly between AD 1750 and 1800. In West and Central Jotunheimen, the outermost moraines of the LIA often date from around AD 1750, whereas in East Jotunheimen, the related moraines tend to be a few decades younger, i.e. date from around AD 1780/1800 (Fig. 2; Winkler, 2002; Matthews, 2005). Owing to the regional ecological conditions (glacier forelands above the tree lines, relatively stable moraine ridges, limited press on lichens by vascular plants and mosses, usually sufficient humidity for lichen growth, siliceous rock types etc.), lichenometry has a comparable high temporal resolution and gives reliable results (Matthews, 2005). The accuracy of lichenometry in dating the LIA maximum in this region are assumed to be within ±20 years for the more recent, sophisticated studies using regional lichen growth curves (e.g. Matthews, 2005).

The AD 1750 LIA maximum in West and Central Jotunheimen is interpreted analogously to the mid-18th century LIA maximum at Jostedalsbreen (Bickerton and Matthews, 1993; Nesje et al., 2008a). The primary climatologic cause for this advance is considered to be increased winter precipitation (Nesje and Dahl, 2003; Nesje et al., 2008a, b; De Jong et al., 2009; Nesje, 2009). By contrast, the second half of the 18th century was dominated by below-average summer temperatures (Winkler, 2001; Nordli et al., 2005). In this period the outlets of Jostedalsbreen retreated slowly from their outermost LIA positions without a major readvance, probably because the drop in summer temperatures was accompanied by low winter precipitation (Bickerton and Matthews, 1993). In Jotunheimen and especially at the most continental

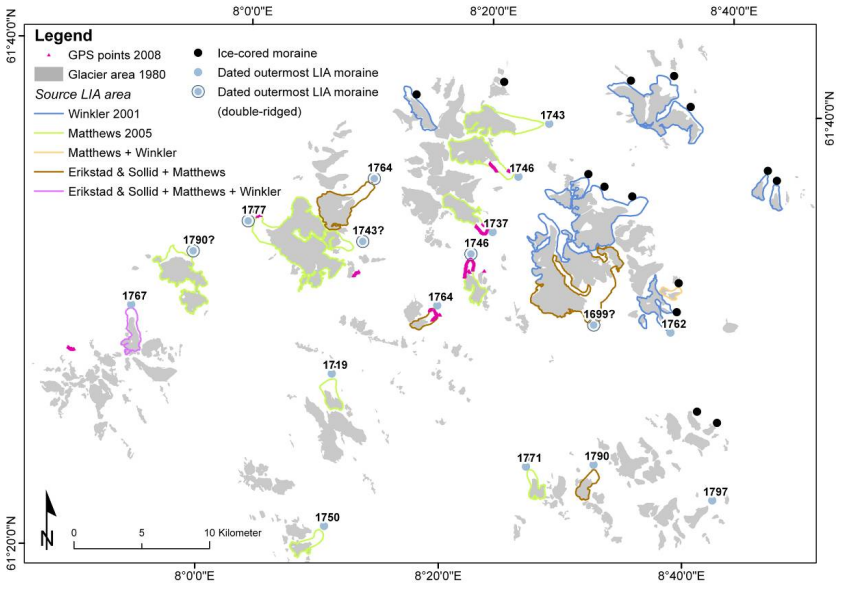

Fig. 2. Available LIA glacier outlines from the geomorphological maps, divided after source. Moraine type and timing of LIA maximum and GPS points of moraine walls measured 2008 are marked. Glacier areas in the 1980s are shown in grey (glacier outline 1980s: Statens Kartverk N50; LIA maximum outlines and timing: Erikstad and Sollid, 1986; Winkler, 2001; Matthews, 2005).

glaciers to the East, however, these climatic conditions were favourable for glacier growth. Therefore, it seems likely that an advance culminating around 1800 in East Jotunheimen overrode all potential older LIA moraines. In the more maritime western and central parts of Jotunheimen, glaciers advanced simultaneously and nearly reached the previous 1750 maximum position, but without overriding and destroying the pre-existing terminal moraine, resulting in double-ridged terminal moraines (with a measurable difference in lichen sizes). The outer ridge is then interpreted to date from the mid-, and the inner ridge from the late 18th century (Winkler, 2002). Double-ridged terminal moraines have not been observed in East Jotunheimen (Winkler, 2001).

We decided to ignore the described variations in the timing of LIA maximum extent of the glaciers in the study region for simplicity reasons. Our following calculations thus assume a uniform LIA maximum at AD 1750. However, when interpreting the climatic causes of the LIA glacier behaviour, it must be emphasized that the timing of the maximum varies with ∼50 years in the region.

4 Material and methods

4.1 Study material

To generate LIA glacier outlines, different data sources were used:

– a satellite image: Landsat 5 TM, Path 199 Row 17, 9 August 2003; cell size 30 m×30 m; cloud cover 0%, with little seasonal snow remaining. The Landsat image delivered by Norsk Satellittdataarkiv was already orthorectified. The orthorectification was tested with 14 check points by the Norwegian Water Resources and Energy Directorate (NVE) (Andreassen et al., 2008);

– 26 aerial photos in 1:40 000 taken in 1966, 1976, and 1981 by Fjellanger Widerøe (Fig. 3). All photos were cloud-free and taken at the end of the ablation season (August/September). In this study, the difference in date was unimportant, because these photos were only used for the purpose of mapping of LIA glacier extent. All photos were original black/white contact copies and had to be orthorectified and georeferenced;

– geomorphological maps containing LIA outlines of totally 25 glaciers, partially including detailed moraine ages (Erikstad and Sollid, 1986; Winkler, 2001; Matthews, 2005) (Fig. 2). These maps have no coordinate system, so some have to be classified as sketches rather as decent maps;

– GPS points for LIA moraine ridges at eight glaciers. This data was collected AD 2008 during field-work using a Garmin eTrex Summit (Fig. 2);

– Digital topographic map in 1:50 000 (called “N50”) with glacier outlines from the AD 1980s by Statens Kartverk (Norwegian mapping authorities);

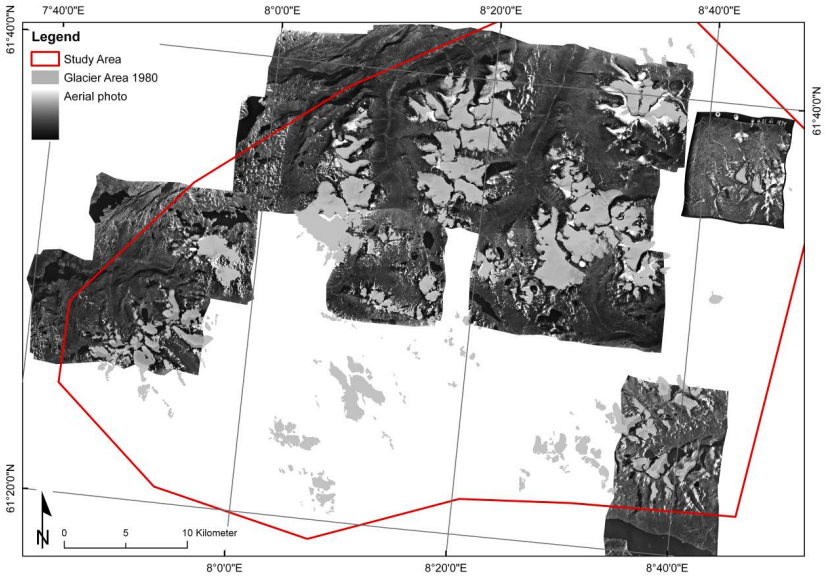

Fig. 3. Coverage of vertical aerial photos available for the study. Glacier area is from the 1980s (aerial photos: Fjellanger Widerøe, 21 July 1966, 1834 B21; 22 August 1976, 5245 J6–8; 29 August 1981, 7084 17–8 44–46; 18–1 4–5, 9, 12–14; 18–2 6–7, 9–13; 18–3 7, 9–11, 13–14; glacier outlines 1980s: Statens Kartverk N50).

- Digital terrain model with 25 m resolution (DTM25) by Statens Kartverk derived from the N50 maps with a root mean square error (RMSE) of 3–5 m;
- digital glacier outlines from AD 2003 with defined identification numbers (IDs) of the glaciers and basins (Andreassen et al., 2008);
- borders of hydrologic basins (called "Regine" watershed); the Regine watersheds have been manually mapped by NVE with N50 as basis.

The digital glacier outlines from 2003 and the 1980s were transferred to glacier areas in GIS. Digitization and calculation were done using GIS-software (ArcGIS 9.2 by *ESRI*). ERDAS IMAGINE 9.1 (by *Leica Geosystems*) was used for orthorectification and georeferencing. All material was converted into the same projection, using Universal Transverse Mercator (UTM) projection in World Geodetic System (WGS) 1984 European datum.

4.2 Mapping LIA area

The glacier outlines for LIA maximum were digitized manually on screen using three different sources: 1) the satellite image, 2) the aerial photos and 3) the geomorphological maps. Glacier outlines from the 1980s and 2003 served as basis for the minimum LIA glacier extent. In the following, we describe the mapping process for each of the three sources.

4.2.1 Landsat image

On a glacier foreland relatively recently deglacierized, vegetation cover is absent or remains sparse. Therefore, the spectral signal is different between the glacier foreland and the area outside (Gao and Liu, 2001; Csatho et al., 2005; Richard and Xiuping, 2006; Albertz, 2007). This spatial pattern can be used for identifying the former LIA glacier covered areas on a satellite image. We displayed the Landsat image as a band 543 composite as red, green, and blue, respectively, and digitized the LIA terminal moraine. The former LIA glacier area was in most cases adequate for manual mapping (Baumann et al., 2008). We also tested (semi-)automatic classification of the glacier foreland, but overlapping spectral signals between forelands and ubiquitous bare rock surfaces in the area made it very difficult to use such classification. Inclusion of other properties in the analysis, e.g. elevation or slope enhanced the result, but not to a convincing degree. Therefore, we decided to digitize the LIA maximum extent manually.

Typical challenges connected to glaciers in cast shadow or with debris cover (Sidjak and Wheate, 1999; Paul, 2001; Kääb et al., 2002; Bolch and Kamp, 2006; Raup et al., 2007) did not cause problems in our study. Shadowed areas were mostly found in the high-altitude accumulation areas and not on the low-lying glacier forelands. Additionally, dealing with cast shadow is easier in manual mapping than in automatic classifications. There were only few glaciers partially debris-covered and mapping of LIA moraines on the glacier foreland was not affected by this.

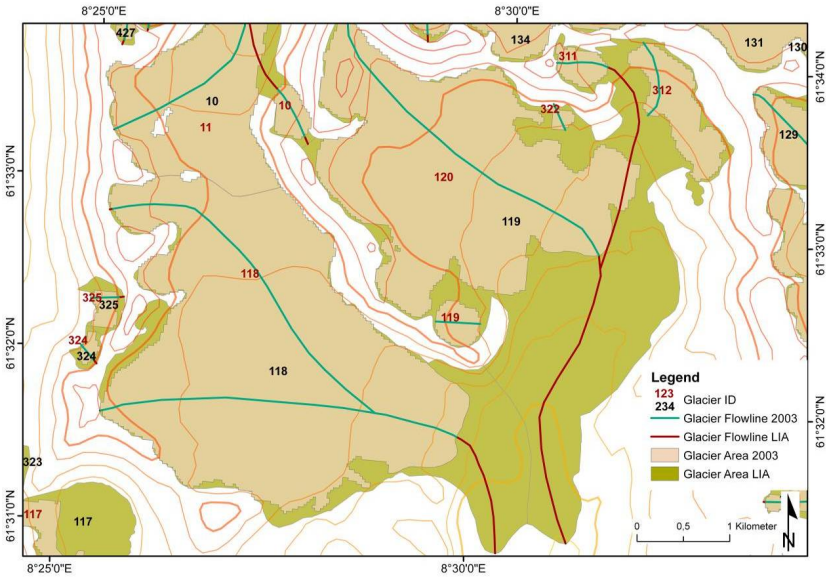

Fig. 4. Vestre (LIA ID=118; black number) and Austre Memurubreen (LIA ID=119) with corresponding flowlines. The separation of Austre Memurubreen since LIA maximum in five single glaciers until 2003 (2003 IDs=119, 120, 311, 312, 322; red numbers) is visible. The flowline on Vestre Memurubreen is divided in two branches. The mean of these branches (highest to lowest elevation) was used. The complete LIA glacier flowline is not visible because of coverage by the 2003 glacier flowline (directly over each other). Elevation contour interval is 100 m. The location of Vestre and Austre Memurubreen is seen in Fig. 1 by letter code MEM (glacier outlines 2003: Andreassen et al., 2008; digital topographic map: Statens Kartverk N50).

4.2.2 Aerial photos

The aerial photos, most of them available in stereo pairs, covered about 50% of the study area and 86% of the glacierized area (based on the glacier extent in the 1980s; Fig. 3). They were georeferenced using the digital topographical map, and orthorectified in ERDAS Imagine using the DTM25 as altitude reference following the procedure for orthorectification as described in the ERDAS manual (ERDAS IMAGINE, 2006). For each photo, four to eight ground control points (GCPs) depending on the fitting of the resulting image were collected. Moraine ridges and the outline of the forelands were used to detect and map the LIA maximum extent. On most glacier forelands the outermost moraines could be mapped fairly well. The outermost moraine ridge was set as LIA maximum due to the almost indisputable absence of older Holocene moraines predating the LIA on the glacier forelands in this region (e.g. Matthews, 1991, 2005; Shakesby et al., 2008).

4.2.3 Geomorphological maps

On the geomorphological maps used in this study, detailed topographical information apart from the moraine ridges was sparse. In consequence, aerial photos were used to georeference and orthorectify them. Although minor problems in orthorectification, the results were considered good enough and LIA maximum extent was manually digitized.

4.2.4 Selection of LIA maximum outline

To derive one final LIA outline per glacier, the different outlines were compared. The outlines of the geomorphological map were assumed to be the most correct and were chosen as the final outline where available (i.e. at 25 glaciers). For all other glaciers, the visibility of the LIA area in the satellite image and aerial photo were compared and the one with the clearest visible boundary was chosen. In cases with substantial deviation between the two outlines, a closer re-check of the sources was made to detect any mapping errors. Only the final outlines were used to calculate the LIA glacier area.

GPS points for the outermost moraine ridges were collected in the field in summer 2008 at eight glaciers. They were collected from (i) five glaciers where a geomorphological map was available, and (ii) three previously unmapped glaciers. The accuracy of the projection of the map in a GIS system as well as the accuracy of the mapping itself could be tested using this data. The difference between the GPS data and the mapping ranged between 0 and 250 m. The mean difference was 41 m with a standard deviation of 83 m. The difference at the unmapped glaciers was 83 m compared with 16 m at the mapped glaciers. This difference might reflect that the mapped glaciers have better visible outermost moraine ridges. Nonetheless, georeferencing and mapping were considered to be satisfactory results for all GPS-mapped glaciers with one exception.

Calculation of glacier area was done using GIS. Since LIA maximum, a large number of the investigated glaciers

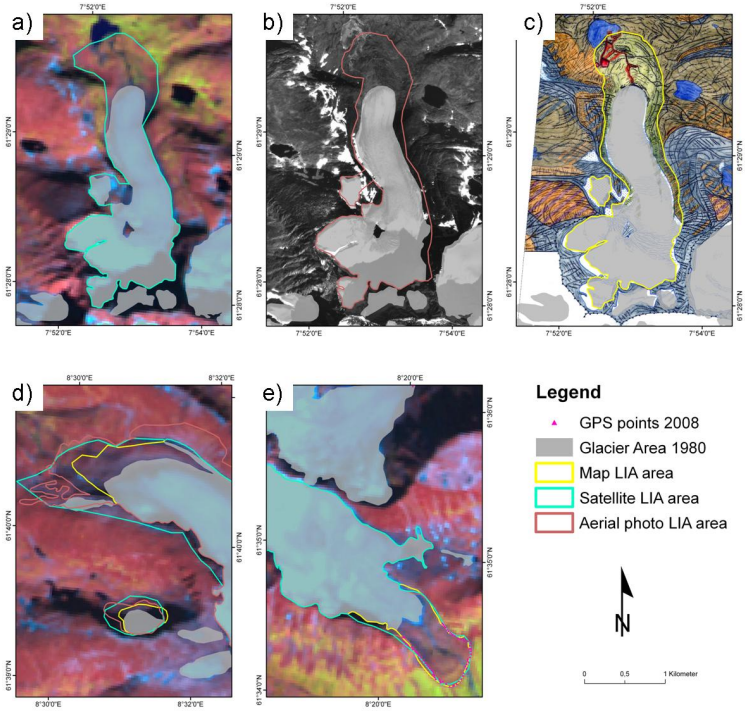

Fig. 5. Mapping of the LIA maximum extent of Styggedalsbreen (STD) on **(a)** the satellite image, **(b)** an aerial photo, and **(c)** a geomorphological map. Overlapping of all three sources for the sensitivity analysis with poor correspondence in **(d)** at Grjotbreen (GRJ) and with good correspondence in **(e)** at Bukkeholsbreen (BUK). Location of the glaciers in Fig. 1 given by letter codes (Satellite image: Norsk Satellittdataarkivet; aerial photo: Fjellanger Widerøe, 29 August 1981, 7084 17–8 46; map: Winkler, 2001; glacier outline 1980s: Statens Kartverk N50).

separated due to glacier retreat and formed individual glaciers. To reconstruct the glaciers at LIA maximum, the present basins were adjusted to fit the formerly larger glacier areas. The LIA basins had to include the transformation of separated glaciers into one basin if they constituted a single glacier during LIA maximum. The boundary of single glacier units at LIA maximum was derived by clipping the LIA maximum extent with the LIA basins and glacier areas were calculated automatically using GIS. Finally, all glaciers smaller than 0.01 km^2 were deleted from the inventory of the glaciers at LIA maximum. At this scale it is difficult to distinguish between glaciers and perennial snowfields (e.g. Paul, 2009). Furthermore, the resolution and accuracy of mapping is restricted by the pixel size of the satellite image. This size class was also not included in the inventory of 2003 (Andreassen et al., 2008).

4.3 Creating LIA centrelines

To calculate glacier lengths during LIA maximum, centrelines were digitized manually using the LIA glacier outlines and the contour lines of N50 as basis. Flowlines were digitized perpendicular to the contour lines, preferably in the middle of the glacier, and from its highest to the lowest points (Paul, 2009). On glaciers with different tributaries or wide accumulation areas, more than one flowline was digitized (e.g. Memurubreen in Fig. 4). In such cases, a mean for the flowlines was calculated and hereafter used as "glacier length". The number of flowlines varied between one and three at individual glaciers.

4.4 Creating LIA inventory data

Inventory data of the glaciers at LIA maximum (LIA inventory) were calculated automatically using ArcGIS and the DTM25. The calculated inventory data included minimum, maximum, and mean altitude, slope, and aspect. Except for aspect, all variables were derived directly from ArcGIS. The aspect was calculated using a routine described in Paul (2007).

4.5 Sensitivity analysis

The glacier outlines were as mentioned derived from three different sources: satellite images, aerial photographs, and geomorphological maps. For 18 glaciers all three sources were available and compared (examples in Fig. 5). The derived areas of all three sources compared well, the coefficient of variation was 1.7%, and all areas were within the 95%-confidencel interval. The differences between the glacier areas from the satellite image and the aerial photos were

Table 1. Classification of the glacier area during LIA maximum into size intervals and comparison with 2003.

Area Interval [km^2]	Number [n]		Number [%]		Mean area [km]		Cumulative [%]	
	LIA	2003	LIA	2003	LIA	2003	LIA	2003
<0.1	26	75	11.16	28.63	0.06	0.06	0.56	2.29
[0.1, 0.5)	96	101	41.20	38.55	0.26	0.24	9.09	14.32
[0.5, 1.0)	37	36	15.88	13.74	0.73	0.72	18.42	27.71
[1.0, 5.0)	63	43	27.04	16.41	2.35	2.20	69.47	76.95
[5.0, 10.0)	8	7	3.43	2.67	6.87	6.40	88.42	100.00
≥10.0	3	–	1.29	–	11.19	–	100.00	100.00
Total	233	262	100	100	1.24	0.87	–	–

small, but mapping using the satellite image revealed a closer agreement to the geomorphological maps than mapping using aerial photos. Both the Landsat image and aerial photos gave larger areas than the geomorphological maps, 1.3 km^2 and 2.2 km^2, respectively, for the total of 18 glaciers, an increase of 0.01 or 0.02%, respectively. In conclusion, the comparison of the mapping sources showed good agreement and the derived LIA glacier outlines were considered to be robust for all three methods.

5 Results

We mapped the LIA maximum extent of 233 glaciers in Jotunheimen with a total area of about 290 km^2 (Fig. 1). The individual parts of composite glaciers and ice caps are here referred to as single glaciers. The mean glacier area was 1.24 km^2. The size distribution of the glaciers is shown in Table 1. Most of the glaciers fall within the interval [0.1, 0.5) km^2, whereas the glaciers in the interval [1.0, 5.0) km^2 exhibit the largest contribution to the total area. Despite a large percentage of the overall number of glaciers (68%), the group of smallest glaciers represents only a minor part of the total glacier area (18%). By contrast, less than 5% of all glaciers (the largest class) constitute more than 30% of the total glacier area. Only three glaciers were larger than 10 km^2 at LIA maximum. The largest glacier in Jotunheimen was Østre Memurubreen with an area of 12.4 km^2.

The maximum altitude of the glaciers ranged between 1500 and 2500 m a.s.l. with a mean of 2010 m a.s.l. (standard deviation (σ)=170 m a.s.l.), the minimum altitude between 1000 and 2400 m a.s.l. with a mean of 1590 m a.s.l. (σ=206 m a.s.l.). The highest elevation range was found on Styggebreen with a range of 1396 m. The minimum, maximum, mean, and median altitude all generally increased from West to East. A relation to the glacier size was only detectable for the minimum altitude. The plot of minimum glacier altitude vs. area (Fig. 6) revealed a lower minimum altitude for larger glaciers than for smaller ones. The coefficient of determination of the best fitting straight line through all points is 0.36. The coefficient of determination for the mean maximum glacier altitudes, shown in the same plot

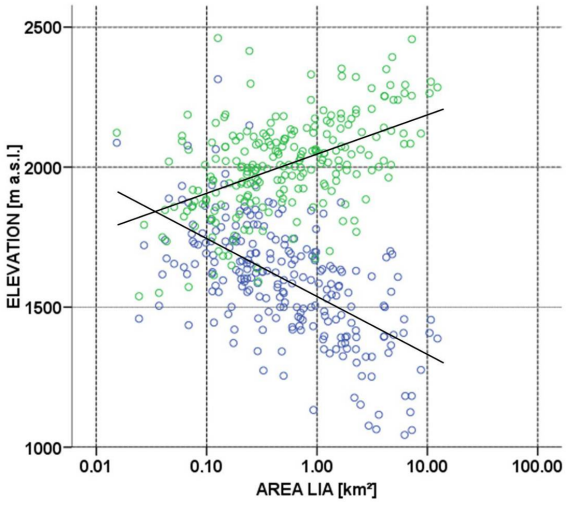

Fig. 6. Scatter plot of minimum (blue dots) and maximum (green dots) elevation vs. LIA glacier area. The solid lines give the best fitting straight line of minimum and maximum elevation, respectively. Note logarithmic horizontal scale.

(Fig. 6), is 0.26. Scatter plots of aspect vs. glacier size and of slope vs. aspect showed no distinct pattern. Furthermore, no relationship was found between the four calculated altitudes (minimum, maximum, mean, and median) and mean aspect or slope.

The length of the glaciers varied between 134 and 6818 m with a mean of 1554 m. About two thirds (65.6%) of the glaciers had lengths shorter than the mean. The median value was 1064 m. More than half of the lengths (50.2%) were in the interval [1.0, 5.0) km (Table 2). Only eight glaciers had a length exceeding 5.0 km, Søre Veobreen had the longest flowline with a length of 6818 m. 41 glaciers (18%) had more than one flowline.

The LIA inventory data were compared with the glacier data from AD 2003. The total area declined from about 290 km^2 during LIA maximum to 190 km^2 in AD 2003 (−35%). The relative area reduction between LIA maximum and 2003 is slightly higher for smaller glaciers than for larger

Table 2. Classification of the glacier length during LIA maximum into length intervals and comparison with 2003.

Length	Number [n]		Number [%]		Mean length [km]	
interval [km]	LIA	2003	LIA	2003	LIA	2003
<0.5	38	92	16.31	35.11	0.33	0.33
[0.5, 1.0)	70	85	30.04	32.44	0.73	0.71
[1.0, 5.0)	117	85	50.21	32.44	2.13	2.08
≥5.0	8	–	3.43	–	6.16	–
Total	233	262	100	100	1.55	1.02

ones, but without indicating any clear pattern. However, the range of change for the smaller glaciers is large (0%–(−100%)). The highest reduction (−47%) is found in the interval [0.1, 0.5) km^2, the smallest (−28%) in the interval [5.0, 10.0) km^2 (Fig. 7). No notable spatial pattern in area reduction could be detected between LIA maximum and 2003 (Fig. 8). The spatial pattern of higher relative area reduction in the northeastern and eastern part of Jotunheimen between the 1980s and 2003 detected by Andreassen et al. (2008) is not visible between LIA and 2003. The calculated hypsography for 100 m intervals of LIA maximum and 2003 (Fig. 9) shows, not surprisingly, a higher absolute area loss at lower elevations. The highest absolute loss occurred at an elevation range of 1500–1700 m a.s.l. The increase in mean elevation (+61 m) is slightly higher than for median elevation (+55 m).

As shown on Fig. 10, a higher number of glaciers smaller than 0.1 km^2 existed in AD 2003, but none larger than 10.0 km^2. Except for these two intervals, the relative distribution of glaciers was similar at both times. In total, 13 glaciers disappeared between LIA and 2003, and 34 glaciers separated into two or more parts.

The four altitude values (minimum, maximum, mean, and median) of LIA maximum were compared with the respective values of 2003. The resulting differences showed neither any spatial pattern nor any relation to glacier size, mean aspect, or slope.

The mean length was reduced by 34% from LIA maximum (1.6 km) to 2003 (1.0 km). The number of glaciers with lengths in the interval <0.5 km decreased from the LIA maximum to 2003 (Table 2). The relative number of glacier length stayed nearly the same in the size interval [0.5, 1.0) km and declined from 50% to 32% in the interval [1.0, 0.5) km.

6 Discussion

6.1 Comparison of sources

For about one third of the aerial photos the accuracy of fitting was not satisfying. Close examination of the sources revealed differences between contour lines from the topographical map (N50) and the DTM25 (mean altitudinal error=3.3 m, σ=12.6 m). Those were possibly related to interpolation errors. To quantify the impact of this difference, several aerial photos were orthorectified again using only the DTM25. The LIA areas digitized with these orthophotos were compared with the first results. The coefficient of determination was close to 1 (r^2=0.9997). Thus, the error regarding the resulting LIA areas could be ignored and errors in orthorectification of the aerial photos were assumed to be negligible. The reported difference in fitting might be caused by the altitude range on each aerial photo (often exceeding 1000 m). The determined deviation is comparable with other studies (e.g. Csatho et al., 2005).

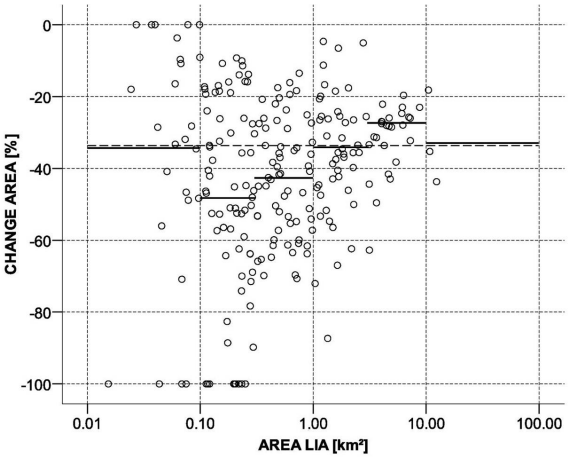

Fig. 7. Scatter plot of relative area change of glacier area between 2003 and LIA vs. LIA glacier area. The solid lines give mean values per size class, the bold dashed line shows the mean for all glaciers (raw data glacier outlines 2003: Andreassen et al., 2008).

In several cases, the geomorphological maps were obviously drawn using non-orthorectified aerial photos. For georeferencing of these maps, aerial photos had to be used. Only on those, the precise position of the moraine ridges could be mapped if no other useful information was available on the maps. Therefore, the geomorphological maps cannot be regarded as an independent source. To determine the potential error emerging during this procedure, the GPS-data collected in field were used. The difference between these GPS-coordinates and the position of the outermost moraine on geomorphological maps was calculated for five glaciers. The mean error of the resulting LIA area is about 28.2 m^2 (σ=8.8 m^2). This error is smaller than the pixel size of the satellite image (30 m×30 m). The RMSE of the georeferenced satellite image itself is about 0.65 pixels, which is about 20 m (Andreassen et al., 2008). The error resulting from topographical inaccuracy of the geomorphological maps is therefore acceptable for our purpose.

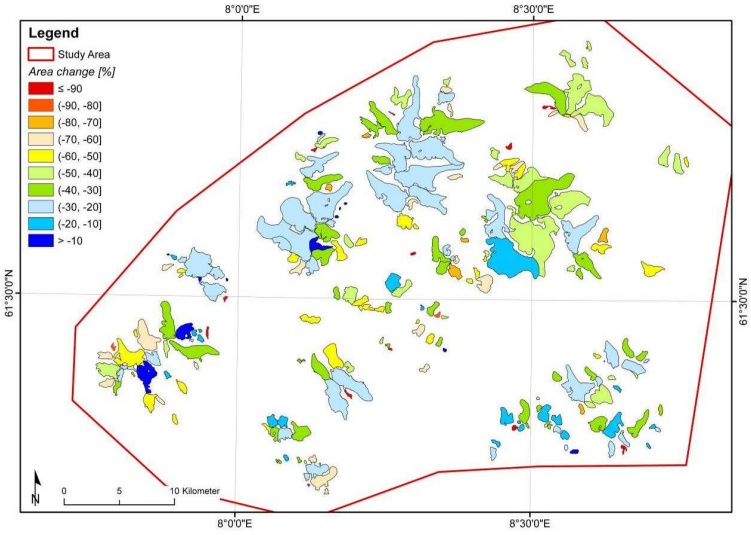

Fig. 8. Colour-coded relative area change between LIA maximum and 2003 for each single glacier. Shown are glacier extents of LIA maximum (raw data glacier outlines 2003: Andreassen et al., 2008).

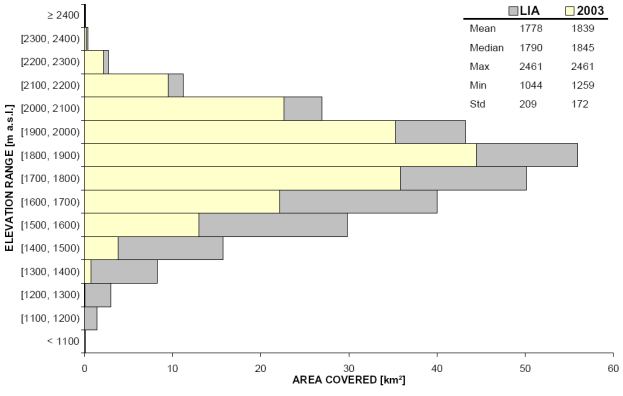

Fig. 9. Glacier hypsography with 100 m contour interval for LIA maximum (grey) and 2003 (yellow) including statistical data. LIA area-altitude distribution is an assumption based on the topographic map of the 1980s (raw data glacier outlines 2003: Andreassen et al., 2008).

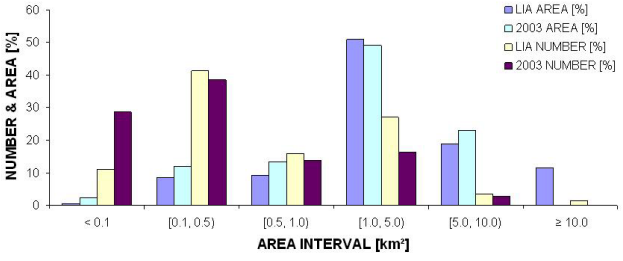

Fig. 10. Comparison of area intervals between LIA maximum and 2003. Both number and area sum are compared (raw data 2003: Andreassen et al., 2008).

6.2 Uncertainties in mapping the LIA maximum

When mapping the LIA maximum outlines the outermost moraine was assumed to represent the maximum glacier extent during LIA. This assumption was based on extensive previous studies (see Sect. 3), but exceptions might be ice-cored moraine systems at few high-altitude cirque glaciers in East Jotunheimen, e.g. at Gråsubreen (Østrem, 1964). Their outermost ridges could pre-date the LIA, although evidence is yet sparse (e.g. Østrem, 1964; Winkler, 2001; Shakesby et al., 2004, 2008). Because of short distances between individual ridges, the possible error by non-exact location of the ridge representing the outermost LIA position within these complex moraine systems are considered to be small. At Gråsubreen, a comparison of the LIA glacier area using six different moraine walls as LIA glacier limit, showed a coefficient of variance of 4.5%.

Another uncertainty is the unknown LIA maximum topography of the glacier which affects the accuracy of the LIA inventory parameters. The slope calculation using the present deglaciated glacier foreland differs from the slope of the former glacier tongue for example. Estimations of mean, median and maximum altitude will also be influenced by the lack of a LIA glacier surface topography. The drainage basins of larger basins might also be different at the LIA maximum, but this is difficult to account for in the analyses. Reconstructions of LIA surfaces could be possible, but will nevertheless be an estimate as no reliable maps are available for validation.

As mentioned in Sect. 4.2, all glaciers smaller than 0.01 km^2 were removed from the inventory because of the uncertainties in mapping. In particular, it is difficult to

distinguish perennial snow patches from small glaciers on that scale (Paul and Andreassen, 2009). Using a larger glacier minimum size revealed that an exclusion of the smallest area interval would, indeed, alter the results. In the original dataset 13 glaciers disappeared between LIA maximum and 2003. Nine glaciers disappeared between LIA and 2003 if all glaciers $<0.1\,km^2$ at LIA maximum are excluded. These nine glaciers ranged between 0.11 and $0.25\,km^2$ at LIA maximum. In relative numbers concerning the total glacier number, 5.6% of the glaciers disappeared with the original dataset and 5.0% with LIA and 2003 area $>0.1\,km^2$.

Mapping should preferably be an objective process with clear rules and a high degree of reproducibility independent of the analyst. In reality, however, different analysts will, as a result of subjective interpretation, never produce the exactly same results (e.g. Andreassen et al., 2008). Therefore, including any kind of objective analysis would be desirable. The test of using supervised or unsupervised image classification was unfortunately not successful in this study.

For the inventory, glacier length was derived by using the mean of all tributaries to compare lengths at the LIA maximum and 2003. The results represent those glaciers as a whole, but the purely theoretical character of this value should be kept in mind as using the mean glacier length suppresses the individual signal of the glaciers. By selecting the maximum flowline, a length that actually is measured on the glacier could have been chosen. But regarding branched flowlines, the change in maximum value for two points of time might cause a change of the corresponding tributary. The flowlines would not longer be identical, and a comparison would be impossible. Changes in the mean value refer to all tributaries and remain, therefore, comparable. Therefore, calculating the mean glacier length from the 1–3 flowlines for each glacier was considered to be an appropriate method for recording LIA glacier lengths.

The mapping of LIA glacier outlines using aerial photos had some limitations. As already mentioned in Sect. 4.2, only 86% of the glacierized area was covered by aerial photos (Fig. 3). Furthermore, due to distortion and displacement towards the edges of the individual photos, the effective working size was even smaller than the whole photo. Finally, it was sometimes difficult to detect the moraine ridges in cases where stereo pairs were missing. A general disadvantage of using aerial photos is the time required for preparation. Each single photo had to be referenced separately. Depending on the number of photos needed to cover the study area, the process of orthorectification and georeferencing of the aerial photos took much longer in total compared with processing the satellite image. Despite multiple use of some GCPs, the processing time was almost the same for each photo. The big advantage of the aerial photos, however, is their high resolution ($0.4\,m \times 0.4\,m$). Objects could be identified very precisely, whereas the resolution of the satellite image ($30\,m \times 30\,m$) is a limiting factor.

6.3 Comparison with other regions

In the following, we compare the LIA results obtained for Jotunheimen with similar inventories from the European Alps, the Southern Alps of New Zealand, and the Canadian Arctic. Unfortunately, no LIA inventory on a regional scale for other glacier regions of Norway is available yet. The European Alps and the Southern Alps of New Zealand have a high-alpine character with mostly individual glaciers similar to Jotunheimen (e.g. Chinn, 2001; Zemp et al., 2008). The glaciers on Cumberland Peninsula of Baffin Island in the Canadian Arctic are also individual glaciers, but mainly of larger sizes (Paul and Kääb, 2005).

The glacier inventory of LIA maximum in Switzerland was compiled by Maisch et al. (2000). The area decrease from AD 1850 (LIA maximum) until 1999 is 3.4% per decade (Paul et al., 2004b), or 51% in total. This decrease is higher than the corresponding one between LIA maximum (AD 1750) and 2003 in Jotunheimen ($\sim$35%; $\sim$1.3% per decade). Glaciers in the two regions Jotunheimen and the Swiss Alps show an asynchronous pattern of the influence of North Atlantic Oscillation (NAO) modes (Nesje and Dahl, 2003), and poorly correlating annual net balances (Günther and Widlewski, 1986; Steiner et al., 2008). Whereas mass balance in southern Norway is well correlated to winter precipitation (Nesje and Dahl, 2003; Matthews and Briffa, 2005), mass balance in the Alps does no show such an impact (Böhm et al., 2007). As a consequence, the increase in temperature affected the European Alps more strongly than Jotunheimen. A higher relative loss at small glaciers also occurred in Switzerland (Paul et al., 2007). Such a difference in relative area decrease depending on glacier size was not detected in Jotunheimen. Whereas 69% of the glacier area in Jotunheimen is due to glaciers $<5\,km^2$, the corresponding figure for the Swiss Alps is only 55% (Zemp et al., 2008). At LIA maximum, a considerably higher amount of glacier area was due to glaciers $>10\,km^2$ in Switzerland (33%) than in Jotunheimen (12%).

A glacier inventory for LIA maximum (AD 1850) exists for the Austrian Alps (Gross, 1987). A second inventory was compiled for AD 1979 (Rott et al., 1993). The glacier area decrease between 1850 and 1969 was 46% (Gross, 1987). This area loss is much higher than calculated for the Swiss Alps (27%) in the comparable period 1850–1973 (Zemp et al., 2008) and for Jotunheimen for the period 1750–2003 (35%). The relative area loss is higher for small glaciers and South and West exposition (Gross, 1987). Glaciers in the Austrian Alps exhibit relatively smaller sizes compared with Jotunheimen, though the maximum extent is higher. The glacier size is possibly the reason for the higher decrease in glacier area as small glaciers will respond more sensitive to changes in climate (Haeberli, 1995; Kuhn, 1995; Böhm et al., 2007).

The Southern Alps of New Zealand are a mountain system with a higher number of individual glaciers (>3000) and a larger total glacier area compared with Jotunheimen (1160 km^2 in AD 1978). New Zealand exhibits a pronounced maritime climate. The mass balance is strongly influenced by atmospheric circulation patterns and correlates well with both the Southern Oscillation Index (SOI) and the Pacific Decadal Oscillation (PDO) mode (Chinn et al., 2005). The glacier inventory data for LIA maximum (owing to the lack of reliable widespread datings set to AD 1850, when many glaciers remained close to their LIA maximum position) were compiled by detection of moraines on vertical aerial photos (Chinn, 1996). A second inventory of the whole region exists for AD 1978. Many of the larger valley glaciers are debris-covered and recently form glacier fronts calving into pro-glacial lakes (Chinn, 1996). During LIA maximum, 67% of the glaciers were in the area class interval [1, 5) km^2 (in total 98% $<5\,km^2$). In 1978, 90% of the glaciers are smaller than $0.5\,km^2$, a shift towards smaller area intervals compared with LIA maximum (M. Hoelzle, personal communication, 2009). The area decrease from LIA maximum until 1978 is 49% (3.9% per decade) (Hoelzle et al., 2007). In the 1980s and 1990s, many debris-free glaciers advanced (Chinn et al., 2005), but retreat continued at most of the debris-covered glaciers, especially where proglacial lakes developed. The debris-covered glaciers with proglacial lakes have generally experienced massive mass loss during recent years (Chinn et al., 2008). The relative area distribution in the Southern Alps and Jotunheimen is similar for LIA maximum. The reduction in glacier area since regional LIA maximum is smaller in Jotunheimen (until 2003) than in the Southern Alps of New Zealand (until 1978). Between 1981 and 2003, many of the larger glaciers in Jotunheimen experienced only small reductions in area. However, glaciers in the eastern and southeastern Jotunheimen had a notable reduction (Andreassen et al., 2008). Maritime glaciers are regarded as highly climate sensitive (Kuhn, 1984; Laumann and Reeh, 1993; Dyurgerov and Meier, 1999). This might explain the differences between the two regions.

LIA maximum glacier extent on Baffin Island in the Canadian Arctic (occurring about AD 1920s; Paul and Kääb, 2005) was mapped by trimline and moraine survey using remote sensing (Paul and Kääb, 2005; Paul and Svoboda, 2009). The glaciers at LIA maximum were larger compared with Jotunheimen, and only 19% were $<5\,km^2$ (Paul and Svoboda, 2009). On Cumberland Peninsula, a part of Baffin Island, there is no scatter towards smaller glaciers and a dependency of relative area change on glacier size (Paul and Kääb, 2005). Since LIA maximum, the glaciers on Baffin Island have lost 13% (1.6% per decade; Paul and Svoboda, 2009), on Cumberland Peninsula 11% (1.4 per decade; Paul and Kääb, 2005). The difference in glacier sizes and climate setting to Jotunheimen limit, however, the value of this comparison.

7 Conclusions

This study showed that satellite imagery and aerial photos could be used for manual mapping of glacier outlines at LIA maximum in Jotunheimen on a regional scale and delivering inventory data of LIA maximum. Glacier flowlines were digitized manually for all glaciers to derive LIA glacier lengths. Challenges occurred during the mapping process (e.g. orthorectification of the aerial photos, combination of the different topographical sources), but the reliability of the mapping results are considered to be satisfactory.

Only a few glaciers vanished completely between LIA and 2003. Overall, the glaciers were larger at LIA maximum, especially at the upper and lower end of the glacier size range. The relative glacier area reduction in Jotunheimen (35%) is not as strong as in other regions (Swiss Alps: 51%; Southern Alps/New Zealand: 49%). It has to be noted that the timing of the LIA maximum differs between the regions.

A comparison of the LIA inventory with the glacier inventories of the 1960s and the 1980s of Jotunheimen could be interesting to study glacier behaviour in relation to changing climate parameters. The methods used here could be applied to map the LIA maximum glacier extent in other regions of Norway.

Acknowledgements. We thank the three reviewers Andreas Kääb, Ian Brown, and Martin Hoelzle for their useful suggestions on a former version of the manuscript, and also Mauri Pelto and Frank Paul for their helpful comments. Remarks and language revision from L. A. Rasmussen (University of Washington) improved the manuscript. This study was supported by a personal grant from the *Bayerischen Graduiertenförderung nach dem Bayerischen Eliteförderungsgesetz* (BayEFG), by a grant for fieldwork in 2008 in Norway from the *Universitätsbund der Universität Würzburg* and a personal grant from the *Qualifikationsprogramm für Wissenschaftlerinnen an der Universität Würzburg*. The study is connected to the DFG-funded project MaMoGla (Grant WI-1701/3) and NVE.

Edited by: J. O. Hagen

References

Albertz, J.: Einführung in die Fernerkundung, 3 ed., Wissenschaftliche Buchgesellschaft, Darmstadt, 2007.

Andreassen, L. M., Elvehøy, H., Kjøllmoen, B., Engeset, R. V., and Haakensen, N.: Glacier mass-balance and length variation in Norway, Ann. Glaciol., 42, 317–325, 2005.

Andreassen, L. M., Paul, F., Kääb, A., and Hausberg, J. E.: Landsat-derived glacier inventory for Jotunheimen, Norway, and deduced glacier changes since the 1930s, The Cryosphere, 2, 131–145, 2008, http://www.the-cryosphere-discuss.net/2/131/2008/.

Baumann, S., Andreassen, L. M., and Winkler, S.: Mapping Little Ice Age glacier maxima in Jotunheimen, using aerial photography and Landsat imagery, Proceedings of EARSeL-LISSIG Workshop on Remote Sensing of Snow and Glaciers in Bern, online available at: http://www.earsel.org/workshops/LISSIG2008/Baumann_Paper.pdf, 2008.

Bickerton, R. W. and Matthews, J. A.: "Little Ice Age" variations of outlet glaciers from the Jostedalsbreen ice-cap, southern Norway: a regional lichenometric-dating study of ice-marginal moraine sequences and their climatic significance, J. Quaternary Sci., 8, 45–66, 1993.

Böhm, R., Schöner, W., Auer, I., Hynek, B., Kroisleitner, C., and Weyss, G.: Gletscher im Klimawandel, Zentralanstalt für Meteorologie und Geodynamik, Wien, 2007.

Bogen, J., Wold, B., and Østrem, G.: Historic glacier variations in Scandinavia, in: Glacier Fluctuations and Climatic Change, edited by: Oerlemans, J., Kluwer Academic Publishers, Dordrecht, 109–128, 1989.

Bolch, T. and Kamp, U.: Glacier Mapping in High Mountains Using DEMs, Landsat and Aster Data, Grazer Schriften der Geographie und Raumforschung, 41, 37–48, 2006.

Bolch, T., Buchroithner, M., Pieczonka, T., and Kunert, A.: Planimetric and volumetric glacier changes in the Khumbu Himal, Nepal, since 1962 using Corona, Landsat TM and ASTER data, J. Glaciol., 54, 592–600, 2008.

Chinn, T.: New Zealand glacier responses to climate change of the past century, New Zeal, J. Geol. Geop., 39, 415–428, 1996.

Chinn, T. J.: Distribution of the glacial water resources of New Zealand, J. Hydrol. (NZ), 40, 139–187, 2001.

Chinn, T. J. H., Salinger, J., Fitzharris, B. B., and Willsman, A.: Glaciers and climate, Bulletin of the Federal Mountain Clubs of NZ 171, 1–15, 2008.

Chinn, T. J. H., Winkler, S., Salinger, M. J., and Haakensen, N.: Recent glacier advances in Norway and New Zealand – a comparison for their glaciological and meteorological causes, Geogr. Ann. A, 87, 141–157, 2005.

Csatho, B. M., van der Veen, C. J., and Tremper, C. M.: Trimline mapping from multispectral Landsat ETM+ imagery, Géographie Physique et Quaternaire, 59, 49–62, 2005.

De Jong, R., Hammarlund, D., and Nesje, A.: Late Holocene effective precipitation variations in the maritime regions of south-west Scandinavia, Quaternary Sci. Rev., 28, 54–64, 2009.

Dyurgerov, M. B. and Meier, M. F.: Analysis of winter and summer glacier mass balance, Geogr. Ann. A, 81, 541–554, 1999.

ERDAS IMAGINE: ERDAS IMAGINE Tour Guides, 730 pp., 2006.

Erikstad, L. and Sollid, J. L.: Neoglaciation in South Norway using lichenometric methods, Norsk Geogr. Tidsskr., 40, 85–105, 1986.

Fægri, K.: Brevariasjoner i Vestnorge i de siste 200 år, Nature, 72, 230–243, 1948.

Gao, J. and Liu, Y.: Applications of remote sensing, GIS and GPS in glaciology: a review, Prog. Phys. Geog., 25, 520–540, 2001.

Gross, G.: Der Flächenverlust der Gletscher in Österreich 1850 – 1920–1969, Zeitschrift für Gletscherkunde und Glazialgeologie, 23, 131–141, 1987.

Günther, R. and Widlewski, D.: Die Korrelation verschiedener Klimaelemente mit dem Massenhaushalt alpiner und skandinavischer Gletscher, Zeitschrift für Gletscherkunde und Glazialgeologie 22, 125–147, 1986.

Haeberli, W.: Glacier fluctuations and climate change detection - operational elements a worldwide monitoring strategy, WMO Bulletin, 44, 23–31, 1995.

Hoel, A. and Werenskiold, W.: Glaciers and snowfields in Norway, Norsk Polarinstitutt, Skrifter, Nr. 114, Oslo University Press, Oslo, 1962.

Hoelzle, M., Chinn, T., Stumm, D., Paul, F., Zemp, M., and Haeberli, W.: The application of inventory data for estimating past climate change effects on mountain glaciers: A comparison between the European Alps and the Southern Alps of New Zealand, Global Planet. Change, 56, 69–82, 2007.

Innes, J. L.: Lichenometry, Prog. Phys. Geog., 9, 187–254, 1985.

IPCC: Climate Change 2007: The Physical Science Basis. Contribution of Working Group I to the Fourth Assessment Report of the Intergovernmental Panel on Climate Change, edited by: Solomon, S., Qin, D., Manning, M., Chen, Z., Marquis, M., Averyt, K. B., Tignor, M., and Miller, H. L., Cambridge University Press, Cambridge, New York, 2007.

Kääb, A., Huggel, C., Paul, F., Wessel, R., Raup, B., Kieffer, H., and Kargel, J. S.: Glacier Monitoring from ASTER Imagery: Accuracy and Applications, in: Proceedings of EARSeL-LISSIG-Workshop Observing our Cryosphere from Space, Bern, 43–53, 2002.

Kargel, J. S., Abrams, M. J., Bishop, M. P., Bush, A., Hamiton, G., Jiskoot, H., Kääb, A., Kieffer, H. H., Lee, E. M., Paul, F., Rau, F., Raup, B., Shroder, J. F., Soltesz, D., Stainforth, D., Stearns, L., and Wessel, R.: Multispectral imaging contributions to global land ice measurements from space, Remote Sens. Environ., 99, 187–219, 2005.

Kuhn, M.: Mass balance imbalances as criterion for a climatic classification of glaciers, Geogr.Ann. A, 66, 229–238, 1984.

Kuhn, M.: The mass balance of very small glaciers, Zeitschrift für Gletscherkunde und Glazialgeologie, 31, 171–179, 1995.

Laumann, T. and Reeh, N.: Sensitivity to climate change of the mass balance of glaciers in southern Norway, J. Glaciol., 39, 656–665, 1993.

Maisch, M., Wipf, A., Denneler, B., Battaglia, J., and Benz, C.: Die Gletscher der Schweizer Alpen: Gletscherhochstand 1850, Aktuelle Vergletscherung, Gletscherschwund, Szenarien, 2 ed., edited by: NFP 31, vdf, Hochschulverlag an der ETH, Zurich, 2000.

Matthews, J. A.: Families of lichenometric dating curves from the Storbreen gletschervorfeld, Jotunheimen, Norway, Norsk Geogr. Tidsskr., 28, 215–235, 1974.

Matthews, J. A.: Families of lichenometric dating curves from the Storbreen gletschervorfeld, Jotunheimen, Norway, Norsk Geogr. Tidsskr., 28, 215–235, 1974.

Matthews, J. A.: Experiments on the reproducibility and reliability of lichenometric dates, Storbreen gletschervorfeld, Jotunheimen, Norway, Norsk Geogr. Tidsskr., 29, 97–109, 1975.

Matthews, J. A.: A lichenometric test of the 1750 end-moraine hypothesis: Storbreen gletschervorfeld, southern Norway, Norsk Geogr. Tidsskr., 31, 129–136, 1977.

Matthews, J. A.: The late Neoglacial ("Little Ice Age") glacier maximum in southern Norway: new ^{14}C-dating evidence and climatic implications, Holocene, 1, 219–233, 1991.

Matthews, J. A.: "Little Ice Age" glacier variations in Jotunheimen, southern Norway: a study in regionally controlled lichenometric dating of recessional moraines with implications for climate and lichen growth rates, Holocene, 15, 1–19, 2005.

Matthews, J. A. and Briffa, K. R.: The 'Little Ice Age': re-evaluation of an evolving concept, Geogr. Ann. A, 1, 17–36, 2005.

Matthews, J. A. and Dresser, P. Q.: Holocene glacier variation

chronology of the Smørstabbtindan massif, Jotunheimen, southern Norway, and the recognition of century- to millennial-scale European Neoglacial Events, Holocene, 18, 181–201, 2008.

Nesje, A.: Latest Pleistocene and Holocene alpine glacier fluctuations in Scandinavia, Quaternary Sci. Rev., 28, 2119–2136, doi:10.1016/j.quascirev.2008.12.016, 2009.

Nesje, A. and Dahl, S. O.: The 'Little Ice Age'- only temperature?, Holocene, 13, 139–145, doi:10.1191/0959683603hl603fa, 2003.

Nesje, A., Bakke, J., Dahl, S. O., Lie, Ø., and Matthews, J. A.: Norwegian mountain glaciers in the past, present and future, Global Planet. Change, 60, 10–27, 2008a.

Nesje, A., Dahl, S. O., Thun, T., and Nordli, Ø.: The "Little Ice Age" glacial expansion in western Scandinavia: summer temperature or winter precipitation?, Clim. Dynam., 30, 789–801, doi:10.1007/s00382-007-0324-z, 2008b.

Nordli, Ø., Lie, Ø., Nesje, A., and Benestad, R.: Glacier mass balance in southern Norway modelled by circulation indices and spring-summer temperature AD 1781–2000, Geogr. Ann. A, 87, 431–445, 2005.

Østrem, G.: Ice-cored moraines in Scandinavia, Geogr. Ann., XLVI, 3, 282–337, 1964.

Østrem, G. and Ziegler, T.: Atlas over breer i Sør-Norge, NVE, Oslo, 1969.

Østrem, G., Dale Selvig, K., and Tandberg, K.: Atlas over breer i Sør-Norge, NVE, Oslo, 1988.

Øyen, P. A.: Isbræstudier i Jotunheimen, Nytt Magasin for Naturvidenskabere, 31, 26–27, 1893.

Paul, F.: Evaluation of different methods for glacier mapping using Landsat TM, in: Proceedings of EARSeL-SIG Workshop Land Ice and Snow, Dresden, 239–245, 2001.

Paul, F.: The New Swiss Glacier Inventory 2000. Application of Remote Sensing and GIS, Schriftenreihe Physische Geographie, Glaziologie und Geomorphodynamik, Geographisches Institut der Universität Zürich, Zurich, 210 pp., 2007.

Paul, F.: Guidelines fort he compilation of glacier inventory data form digital sources, GLIMS, online available at: http://globglacier.ch/docs/guidelines_inventory.pdf, 2009.

Paul, F. and Andreassen, L. M.: Creating a glacier inventory for the Svartisen region (Norway) from Landsat ETM+ satellite data: Challenges and results, J. Glaciol., 55, 607–618, 2009.

Paul, F. and Kääb, A.: Perspectives on the production of a glacier inventory from multispectral satellite data in Arctic Canada: Cumberland Peninsula, Baffin Island, Ann. Glaciol., 42, 59–66, 2005.

Paul, F. and Svoboda, F.: A new glacier inventory on southern Baffin Island, Canada, from ASTER data: II. Data analysis, glacier change and applications, Ann. Glaciol., 50, 22–31, 2009.

Paul, F., Huggel, C., and Kääb, A.: Combining satellite multispectral image data and a digital elevation model for mapping debris-covered glaciers, Remote Sens. Environ., 89, 510–518, 2004a.

Paul, F., Huggel, C., Kääb, A., Kellenberger, T., and Maisch, M.: Comparison of TM-derived glacier areas with higher resolution data sets, in: Proceedings of EARSeL-LISSIG-Workshop Observing our Cryosphere from Space, Bern, 15–21, 2003.

Paul, F., Kääb, A., and Haeberli, W.: Recent glacier changes in the Alps observed by satellite: Consequences for future monitoring strategies, Global Planet. Change, 56, 111–122, 2007.

Paul, F., Kääb, A., Maisch, M., Kellenberger, T., and Haeberli, W.: Rapid disintegration of Alpine glaciers observed with satellite data, Geophys. Res. Lett., 31, L21402, doi:10.1029/2004GL020816, 2004b.

Raup, B., Kääb, A., Kargel, J. S., Bishop, M. P., Hamiton, G., Lee, E., Paul, F., Rau, F., Soltesz, D., Khalsa, S. J. S., Beedle, M., and Helm, C.: Remote sensing and GIS technology in the Global Land Ice Measurements from Space (GLIMS) Project, Comput. Geosci., 33, 104–125, 2007.

Richard, J. A. and Xiuping, J.: Remote Sensing Digital Image Analysis. An Introduction, 4 ed., Springer Verlag, Berlin, 2006.

Rott, H., Scherler, K. E., Reynaud, L., Barbero, R. S., and Zanon, G.: Glaciers of Europe - Glaciers of the Alps, in: Satellite Image Atlas of glaciers of the World, edited by: Williams, R. S. J. and Ferringo, J. G., USGS Professional Paper 1386-E-1, USGS, 1993.

Shakesby, R. A., Matthews, J. A., and Schnabel, C.: Cosmogenic ^{10}Be and ^{26}Al ages of Holocene moraines in southern Norway II: evidence for individualistic responses of high-altitude glaciers to millennial-scale climatic fluctuations, Holocene, 18, 1165–1177, 2008.

Shakesby, R. A., Matthews, J. A., and Winkler, S.: Glacier variations in Breheimen, southern Norway: relative-age dating of Holocene moraine complexes at six high-altitude glaciers, Holocene, 14, 899–910, 2004.

Sidjak, R. W. and Wheate, R. D.: Glacier mapping of the Illecillewaet icefield, British Columbia, Canada, using Landsat TM and digital elevation data, Int. J. Remote. Sens., 20, 273–284, 1999.

Solomina, O., Barry, R., and Bodnya, M.: The retreat of tien shan glaciers (Kyrgyzstan) since the Little Ice Age estimated from aerial photographs, lichenometric and historical data, Geogr. Ann. A, 86, 205–215, 2004.

Statens Kartverk: Galdhøpiggen, Norway, Statens Kartverk, Oslo, 1985.

WGMS: Global Glacier Changes: facts and figures, edited by: Zemp, M., Roer, I., Kääb, A., Hoelzle, M., Paul, F., and Haeberli, W., UNEP, World Glacier Monitoring Service, Zürich, 88 pp., 2008.

Winkler, S.: Untersuchungen zur Klima- und Morphodynamik in skandinavischen Gebirgsregionen während des Holozän – ein Vergleich ihrer Wechselwirkungen und Prozeßsysteme im überregionalen Kontext kaltgemäßigter maritimer Gebirgsregionen, Habilitation thesis, Fachbereich Geographie/Geowissenschaften, Universität Trier, Trier, 2001.

Winkler, S.: Von der "Kleinen Eiszeit" zum "globalen Gletscherrückzug". Eignen sich Gletscher als Klimazeugen?, Colloquia Academia, Abhandlungen der Mathematisch-naturwissenschaftlichen Klasse 2002 Nr. 3, Akademie der Wissenschaften und der Literatur Mainz/Franz Steiner Verlag Stuttgart, 2002.

Winkler, S.: Gletscher und ihre Landschaften – eine illustrierte Einführung, Wissenschaftliche Buchgesellschaft Darmstadt, 2009.

Wolken, G. J.: High-resolution multispectral techniques for mapping former Little Ice Age terrestrial ice cover in the Canadian High Arctic, Remote Sens. Environ., 101, 104–114, 2006.

Zemp, M., Paul, F., Hoelzle, M., and Haeberli, W.: Glacier fluctuations in the European Alps 1850-2000: an overview and spatio-temporal analysis of available data, in: The darkening peaks: Glacial retreat in scientific and social context, edited by: Orlove, B., Wiegandt, E., and Luckman, B., University of California Press, 2008.